Synchronization and spatiotemporal self-organization in the NO+CO reaction on Pt(100). II. Synchronized oscillations on the hex-substrate

Cite as: J. Chem. Phys. **100**, 8492 (1994); https://doi.org/10.1063/1.466747
Submitted: 05 November 1993 • Accepted: 16 February 1994 • Published Online: 31 August 1998

G. Veser and R. Imbihl

Synchronization and spatiotemporal self-organization in the NO+CO reaction on Pt(100). II. Synchronized oscillations on the hex-substrate

G. Veser and R. Imbihl
Fritz-Haber-Institut der Max-Planck-Gesellschaft, Faradayweg 4-6, D-14195 Berlin, Germany

(Received 5 November 1993; accepted 16 February 1994)

The NO+CO reaction exhibits sustained rate oscillations on Pt(100) under conditions where the surface is mostly hex-reconstructed. These rate oscillations have been investigated in the 10^{-6} mbar range using photoemission electron microscopy as a spatially resolving method. During the rate oscillations which appear in a temperature-window ranging from 490 to 478 K, the surface reacts in a spatially homogeneous way. At the upper T-boundary of the oscillatory range, the oscillations develop via a Feigenbaum scenario leading from chaotic small amplitude oscillations at high T to regular period-1 oscillations at lower T. At the lower T-boundary of the oscillatory range, at $T=478$ K, target patterns appear, causing the collapse of the amplitude of the rate oscillations. As the temperature is lowered further, the parallel wave trains become increasingly irregular. Spiral waves form, and finally one observes only local reaction outbursts. A model for the synchronization mechanism in the rate oscillations is proposed based on the $1\times1\Leftrightarrow$hex-phase transition, while the origin of the chaotic oscillations in this reaction system is discussed in terms of a transition from unsynchronized to synchronized oscillations.

I. INTRODUCTION

The NO+CO reaction on Pt(100) has already been the subject of a number of investigations.[1–11] These studies first focused onto the overall kinetics and the mechanism of the rate oscillations and led to a mathematical model that could reproduce the major experimental findings.[3,5] With the introduction of photoemission electron microscopy (PEEM) as a spatially resolving method, a variety of spatiotemporal patterns was found in the NO+CO reaction on Pt(100), which were then the aim of detailed investigations.[6–9] In these studies, however, only damped rate oscillations were reported, i.e., after excitation by a small T perturbation ($\Delta T<5$ K) the amplitude of the rate oscillations decayed after a small number of cycles.

By applying special care to the preparation of the surface during the present investigations, it was also possible for the first time to obtain sustained rate oscillations in the NO+CO reaction on Pt(100). These sustained rate oscillations occur at elevated temperatures ($T>478$ K) under conditions where the surface is mostly hex reconstructed. As demonstrated by PEEM, these oscillations proceed spatially homogeneously. In contrast to this behavior, a second T-window for oscillations exists, located at lower temperature, in which the oscillations take place unsynchronized on a pure 1×1 substrate.[3,6,9] Due to the absence of long range coupling, the surface oscillates only on a local scale without exhibiting macroscopic rate oscillations. Thus, two T-windows for oscillations exist in Pt(100)/NO+CO, which have entirely different behavior with respect to synchronization.

While spatial pattern formation in the lower-lying T-window for oscillations has already been the subject of part I of this report,[9] the present paper focuses entirely on the rate oscillations in the upper T-window. In this oscillatory window one finds two remarkable transitions, a Feigenbaum scenario at the upper T-boundary, leading from chaotic oscillations to stable period-1 oscillations, and a discontinuous breakdown of the rate oscillations at the lower T-boundary, leading from a synchronized oscillating surface to spatiotemporal pattern formation.[10]

As will be shown, these experimental findings can be discussed in the context of a global coupling mode, which synchronizes the oscillating surface, and which is transmitted via partial pressure changes in the gas-phase. The breakdown of this global coupling mode gives rise to different kinds of transitions which can be observed in the experiments and which will be discussed qualitatively here. The experimental investigations are, however, also complemented by mathematical modeling.[10] In particular, we attempt to simulate the different synchronization behavior in the two existence ranges for oscillations. These simulations are currently underway and the results will be published in a subsequent paper.

II. EXPERIMENT

The experiments were all carried out in a standard stainless steel ultrahigh vacuum (UHV) chamber of about 80 ℓ volume which was operated as an isothermal, gradient-free flow reactor. The chamber could be pumped down to a base pressure of $p\leqslant2\times10^{-10}$ mbar by a combination of a 360 ℓ/s turbomolecular pump, an ion getter pump, and a titanium sublimation pump. The system was equipped with facilities for low energy electron diffraction (LEED), Auger electron spectroscopy (AES), a Kelvin probe for work function measurements, and two quadrupole mass spectrometers (QMS), one of which was differentially pumped, for measuring partial pressures under reaction conditions.

For PEEM measurements, ultraviolet (UV) light from a deuterium discharge lamp (30 W, Ealing) with a maximum emission between 5.2 and 6.2 eV photon energy could be focused into a spot of ≈1 mm^2 onto the single crystal.[12] The ejected photoelectrons were focused by means of the electrostatic three lens electron optics of the PEEM, amplified by a

 0021-9606/94/100(11)/8492/9/$6.00

channel-plate electron multiplier, and imaged onto a phosphorous screen. These images were then recorded with a charge-coupled device (CCD)-camera and stored on a videotape. This allows for an imaging of the spatial work function distribution on the sample surface with a lateral resolution of ≈ 1 μm at the video frequency of 50 Hz. The microscope could be differentially pumped by a 170 ℓ/s turbomolecular pump, thereby reducing the pressure at the channel plate by roughly two orders of magnitude with respect to the pressure in the main chamber under reaction conditions.

The two Pt(100) samples (dimensions $\approx 5\times 5$ mm^2, ≈ 1 mm thickness) were cleaned by standard methods involving repeated cycles of oxidation and Ar-ion sputtering prior to each experiment. For the experiments, high purity gases were used (purity, CO 4.7; NO 2.8; both LINDE), which were introduced into the chamber via a feedback controlled gas-inlet system, ensuring a constant flow rate of the reacting gases within $\leq 1\%$ precision. The partial pressures given in this report have been corrected for the different ion gauge sensitivities of the respective gases, i.e., $S_{CO}/S_{N_2} = 1.0$ and $S_{NO}/S_{N_2} = 0.8$ were used as correction factors.

For the measurements of the Feigenbaum-scenario (the period doubling cascade), an optimum control of the sample temperature turned out to be of central importance. This was realized by spotwelding a NiCr/Ni-thermocouple to the back of the crystal and controlling the heating current by means of a PID-control unit, that was recalibrated prior to each experiment. This allowed us to keep the temperature fluctuations below 0.05 K over the typical duration of 30 min for recording a time series.

III. RESULTS

A. Bifurcation diagram

Figure 1 gives an overview of the high-temperature range for rate oscillations and of the various types of spatiotemporal patterns that can be observed under oscillatory and under stationary reaction conditions. The complete existence range for oscillatory behavior in the NO+CO reaction on Pt(100) has been mapped out in (p_{NO},T)-parameter space (p_{CO}=const.).[9] The bifurcation diagram in Fig. 1 has been recorded in the direction of decreasing temperature, i.e., after heating the sample up to 800 K, the hex-reconstructed surface was cooled down in a mixed NO/CO atmosphere.

In the NO reduction with CO on Pt(100), two stable branches of the reaction kinetics exist, with the less active one being associated with the hex-phase and the more active one with the 1×1 phase of Pt(100).[2,3,11] The different activities of the two surfaces are due to the fact that NO dissociates readily on the 1×1-substrate while the hex-phase is quite inefficient in that respect.[3,13] The two rate branches give rise to a hysteresis in the reaction rate upon cycling the temperature as shown in Fig. 2. The diagram demonstrates that the existence range for oscillations (only the upper range is shown here) is located in a transition region where the NO/CO-induced lifting of the hex reconstruction restores the high level of catalytic activity that is associated with the 1×1-phase.[3,14,15]

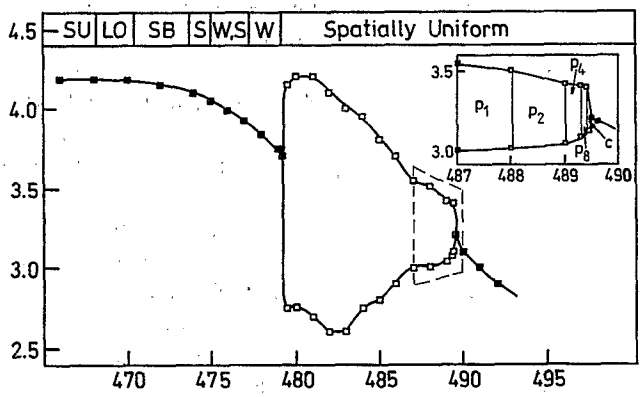

FIG. 1. Bifurcation diagram showing the range where the CO_2 production rate r_{CO_2} is stationary (filled squares) and where the reaction rate exhibits kinetic oscillations. The oscillation amplitude, i.e., the upper and lower turning points, are marked by open squares. The upper and lower T-boundaries of the rate oscillations are refered to as T_1 and T_2 in the text, with T_1=489.6 K and T_2=478 K. The inset shows the the Feigenbaum scenario, which is found at the upper T-boundary of the oscillatory range. The different types of spatial patterns, which can be observed in PEEM, are indicated schematically. SU=spatially uniform, W=wave trains, W,S=wave trains and spirals, S=spirals, SB=spiral breakup, and LO=local outbursts. The experiments were conducted in the direction of decreasing T with $p_{NO}=4\times10^{-6}$ mbar and $p_{CO}=4\times10^{-6}$ mbar.

Within the oscillatory range, no hysteresis occurs and the oscillation amplitude is independent of the direction in which the temperature is varied. The discontinuous transition at the lower T-boundary, T_2=478 K, of the oscillatory range is also not associated with any detectable hysteresis effects, but irreversible changes occur, if the temperature is decreased by more than ≈ 1 K below T_2. In that case, a hysteresis occurs as the reaction rate moves onto the upper rate branch upon increasing the temperature again and resides there during further heating.

The above results indicate that the 1×1⇔hex surface phase transition (SPT) is reversible as long as the amount of structural change is small as is the case inside the oscillatory window. However, the structural changes become irreversible as soon as a larger portion of the hex-phase is converted into the 1×1-phase. From previous LEED experiments one

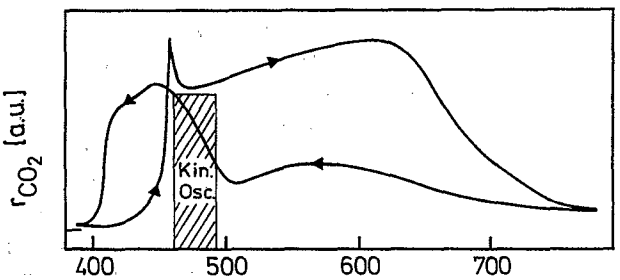

FIG. 2. Reaction rate hysteresis as found in temperature cycling experiments in the NO+CO reaction on Pt(100). Of the two oscillatory ranges, only the one located at higher T is indicated in the diagram. Experimental conditions were $p_{NO}=4\times10^{-6}$ mbar and $p_{CO}=2\times10^{-6}$ mbar. A heating rate of 0.1 K/s was applied.

can estimate that this threshold lies below 30% of the surface area.[3] The present PEEM observations are in qualitative agreement with this value, since under oscillatory conditions, the intensity changes in PEEM are extremely small. This indicates that the maximum amount of reconstructed surface that is lifted under oscillatory conditions may even be well below 30% of the total surface area.

During rate oscillations, the surface reacts spatially homogeneously. The term spatially homogeneous here means homogeneous on the macroscopic length scale (>1 μm) which is resolvable by PEEM measurements. On a microscopic length scale, however, spatial nonuniformities such as adsorbate islands may exist and, as will be shown further below, this is evidently the case in the system considered here. In PEEM, one observes uniform intensity changes, with the maximum intensity coinciding with the rate maximum while the minimum intensity falls upon the rate minimum. Since the hex-reconstructed surface exhibits a lower work function than the adsorbate covered 1×1-phase (assuming CO is in excess)[3,14,15] the same phase relationship between surface structure and CO_2 production is established that has previously been observed in LEED measurements.[3] The maximum in catalytic activity correlates with the maximum in hex reconstruction and vice versa.

In the upper T-window for oscillations, spatial patterns can only be observed if CO is present in excess, i.e., for $p_{NO} \leq p_{CO}$.[9] If this condition is met, pattern formation occurs in the T-range below T_2 where the rate oscillations have already vanished. The discontinuous transition at T_2 is thus associated with the emergence of spatial patterns, i.e., with a transition from purely temporal to spatiotemporal oscillations. In the following, we will first discuss those results that relate to a spatially homogeneously oscillating surface, before then proceeding to a discussion of the spatiotemporal patterns below T_2. For this reason, the Feigenbaum scenario at the upper T-boundary of the oscillations is discussed first, since the surface is oscillating uniformly during this transition.

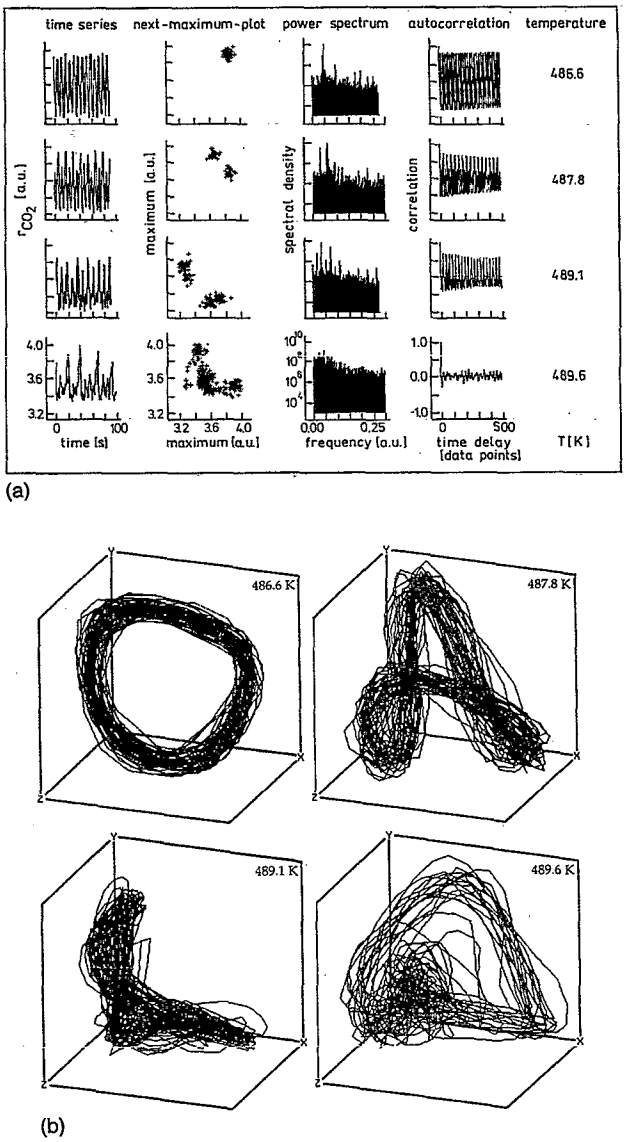

FIG. 3. The Feigenbaum scenario as observed in macroscopic rate measurements at the high-T boundary of the oscillatory region. (a) Time series with corresponding power spectra, next-maximum plots, and autocorrelation functions, and (b) the corresponding attractors in phase space, reconstructed with Taken's delay method from the data shown in (a). The axes are $x=x(t)$, $y=x(t+\tau)$, $z=x(t+2\tau)$, with τ being the delay time.

B. The Feigenbaum scenario

At the high T-boundary of the oscillatory range, the rate oscillations develop as aperiodic rate variations whose amplitude grows continuously with increasing distance from the temperature $T_1 \approx 489.6$ K, which represents the upper T-boundary for rate oscillations. Upon further decreasing the temperature, the rate oscillations undergo a reverse sequence of period-doublings leading from the aperiodic oscillations at high temperature to stable period-1 oscillations at lower temperature. This scenario is depicted in the inset of Fig. 1. The corresponding time series, power spectra, next-maximum plots, and autocorrelation functions are displayed in Fig. 3.

One notes that the noise level in the rate measurements in Fig. 3(a) is relatively high which can be attributed to the use of a differentially pumped mass spectrometer with a high background level of CO_2. However, in the time series and in the power spectra oscillations with period-2 and period-4 are clearly identifiable and even period-8 oscillations could be made out in some time series. The whole scenario is completely reversible and exactly reproducible with respect to the bifurcation points. This behavior suggests that the transition from aperiodic to regular oscillations obeys a Feigenbaum scenario. This interpretation is also supported by the scaling of subsequent bifurcation points. From the first two period doubling temperatures, one calculates a value of $d=5 \pm 0.5$ for the first Feigenbaum constant that is in reasonable agreement with the theoretical value $d=4.669\ldots$.[16]

With regard to the bad signal to noise ratio of the data, we did not attempt to go through a detailed analysis of the aperiodic data as it has been done for Pt(110)/CO+O_2, i.e., determining the embedding dimension, the Lyapunov exponents, etc.[17,18] The existence of a Feigenbaum scenario, however, strongly supports the suggestion that the aperiodic time

series discussed here represent deterministic chaos. This is further confirmed by the following observations. The power spectrum for $T=489.6$ K shown in Fig. 3(a) displays a broad maximum as it is expected for chaotic behavior. The autocorrelation function for the corresponding time series, which is included in Fig. 3(a), decays quite rapidly, while the autocorrelation functions for the periodic data, which are also shown in the diagram, exhibit a nondecaying oscillatory behavior for longer times. Most notably, the next-maximum plot of the chaotic time series as given in the same plot shows a single peaked distribution which has been shown to be characteristic for deterministic chaos.[19]

From the time series measured during the Feigenbaum scenario, 3D-attractors have been reconstructed using Taken's delay method with the delay time $\tau=T/3$, where T is the period of the oscillations.[20] This delay time was determined by starting with the value at which the autocorrelation function displays its first zero and then varying τ until the largest extension of the attractor is found by visual inspection. The resulting attractors for period-1, period-2, period-4, and the chaotic oscillations are displayed in Fig. 3(b). Despite the relatively high noise level, which washes out the detailed structure, one can observe the unfolding of the attractor, which fills out more and more of the available phase space as the oscillations become chaotic.

C. Breakdown of global coupling

Upon decreasing the temperature starting from T_1, the amplitude of the rate oscillations increases continuously until at T_2 the rate amplitude collapses in a discontinuous transition (see Fig. 1). PEEM measurements conducted parallel to the recording of the reaction rate show, that simultaneously with the breakdown of the rate oscillations, spatial pattern formation occurs on the catalyst surface. Periodic wave trains with a spatial periodicity of ≈ 70 μm and a velocity of ≈ 5 μm/s appear in PEEM. As demonstrated in Figs. 4(a) and 4(b), these waves emanate from structural imperfections of macroscopic size (typically 1–5 μm diam) and from the border region of the single crystal, which is always structurally less perfect than the rest of the surface.

The transition from the uniformly oscillating surface to the wave patterns has been investigated in some detail and, within the experimental accuracy of ≈ 0.25 K, the transition always occurred discontinuously. Furthermore, no hysteresis effects were detectable if T was not decreased by more than ≈ 1 K below T_2. Since the homogeneously oscillating surface can only be synchronized via gas-phase coupling, we can associate the collapse of the rate oscillations with the breakdown of gas-phase coupling. The efficiency of this coupling mode in the rate oscillations can be demonstrated quite easily by applying an external perturbation to the partial pressures, which is of the same magnitude as the partial pressure variations generated by the rate oscillations within the system itself (typically 1% of p_{CO} and p_{NO}). The periodic forcing experiments show, that the system already responds to a very small forcing amplitude of the order of less than 1% of p_{CO}, thus confirming the efficiency of gas-phase coupling. In contrast to this external modulation, the self-generated partial pressure variations during the macroscopic

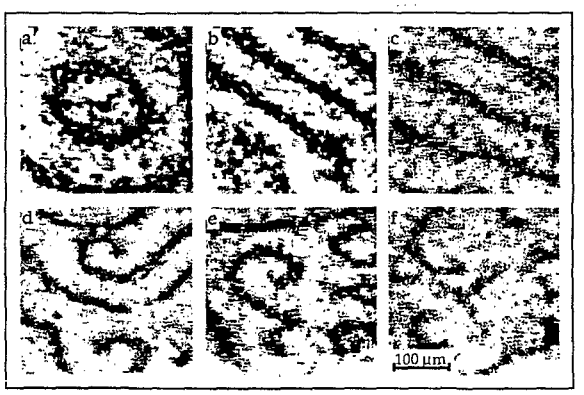

FIG. 4. Sequence of PEEM images demonstrating various stages of spatial pattern formation after the breakdown of global coupling as schematically indicated in Fig. 1. (a) Surface defect and (b) defective border region emitting waves at $T=478$ K; (c) parallel wave trains, $T=477.5$ K; (d) break-up of wave trains and formation of spiral waves, $T=475.5$ K; (e) spiral waves at $T=474.5$ K; and (f) local outbursts at $T=472$ K. The size of the frames is 300×300 μm^2. Experimental conditions were $p_{NO}=4\times10^{-6}$ mbar and $p_{CO}=4\times10^{-6}$ mbar.

rate oscillations arise due to mass balance in the reaction. Since the reaction rate integrates over all local reactivities, gas-phase coupling represents a global interaction in the oscillating system.

In order to follow the collapse of the rate oscillations in more detail, we look at the temporal evolution of this process depicted in Fig. 5. This plot shows the decay of the rate oscillations after the final temperature adjustment has brought T below T_2. The same diagram also displays the temporal evolution of the PEEM intensity integrated in windows of varying size. One notes that the intensity variations in the large windows damp out in the same way as the reaction rate, while the oscillations in the small windows retain a constant oscillation amplitude even after the collapse of the rate oscillations. One also realizes that during the transition from synchronized to local oscillations the oscillation frequency increases by almost a factor of 2. Interestingly this frequency increase does not take place continuously but occurs within only two or three oscillation cycles at the moment when the global oscillations have almost ceased to exist.

The temperature dependence of the local oscillation frequency (being equal to the global oscillation frequency in the case of the rate oscillations) is displayed in Fig. 6 for the whole temperature range spanned by the bifurcation diagram in Fig. 1. Above and below the frequency jump at T_2, the frequency varies linearly with temperature, but this linear dependence exhibits two different slopes above and below T_2, pointing to the existence of two different populations of oscillators. Since the local oscillation frequency below T_2 is determined by defects sending out waves, we can assign the less steep slope below T_2 to these defects, while we can associate the steeper slope above T_2 with oscillations on the defect free surface ("bulk").

With the assignments just given, the breakdown of global coupling can now be explained in a qualitative way using the plot in Fig. 6. Above T_2, both defects and the bulk os-

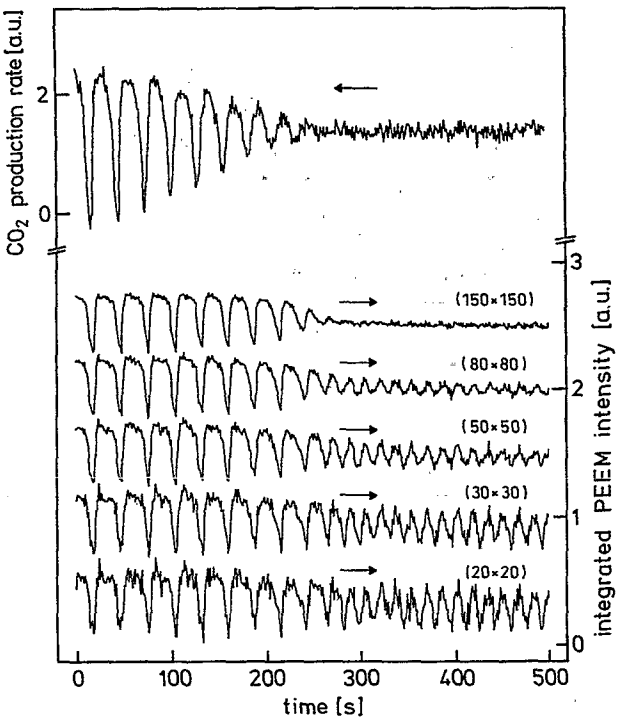

FIG. 5. Decay of the rate oscillations and behavior of the local intensities in the PEEM images (corresponding to local reaction rates) after adjustment of the critical temperature $T=478$ K. The local intensities have been determined by integrating the intensity in small areas in the PEEM images, the size of which is indicated in μm by the numbers at the corresponding curve. Experimental conditions were $p_{NO}=4\times10^{-6}$ mbar and $p_{CO}=4\times10^{-6}$ mbar.

cillate with the same frequency synchronized by gas-phase coupling. With decreasing temperature, the difference in frequency between defects and bulk becomes increasingly larger, until gas-phase coupling is no longer strong enough to enforce complete synchronization. Some defects become supercritical and start to emit waves. As the frequency of the defect oscillations is higher than the frequency of the bulk oscillations, the waves that are emitted by the defects will be able to propagate over the catalyst surface. Furthermore, since a region filled with periodic waves no longer contributes to the amplitude of the rate oscillations, the strength of the global coupling mode will decrease. This gives rise to a positive feedback between the spreading of the waves and the disappearance of gas-phase coupling, thus explaining the abruptness of the transition.

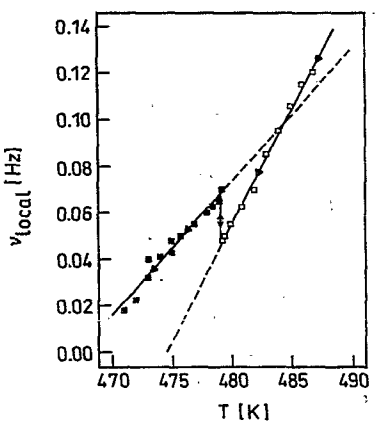

FIG. 6. Variation of the global (open squares) and local (filled squares) oscillation frequency ν_{local} in the bifurcation scenario depicted in Fig. 1. While the global frequencies have been taken from measurements of the reaction rate with mass spectrometry, the local frequencies have been determined by integrating the intensity in a small area of 20×20 μm^2 size in the PEEM images. Experimental conditions were $p_{NO}=4\times10^{-6}$ mbar and $p_{CO}=4\times10^{-6}$ mbar.

Based upon the observation that an extensive preparation procedure is necessary in order to obtain sustained rate oscillation in Pt(100)/NO+CO, one could suspect that structural imperfections are also responsible for the damping effect present with rate oscillations on less well-prepared surfaces. This hypothesis was tested by exposing a Pt(100) surface, which before had been shown to exhibit sustained oscillations to a mild sputtering treatment ($p_{Ar}=2\times10^{-7}$ mbar, $T=500$ K, $E=800$ eV, $t=3$ min). After this treatment, the surface indeed showed damped rate oscillations as had been observed in earlier experiments.[2,3] Since sputtering creates only microscopic defects on the surface, such microscopic defects seem to be responsible for the damping effect. One therefore has to conclude that in addition to macroscopic defects, even microscopic defects can have a desynchronizing influence on the oscillations in the NO+CO reaction.

D. Spatial pattern formation

As indicated in Fig. 1, various stages of spatiotemporal pattern formation can be observed in the temperature range below T_2, before at 469 K a homogeneous stable state is again reached. PEEM images illustrating these stages are displayed in Fig. 4. Directly after the collapse of the rate oscillations, target patterns are seen in PEEM with large defects playing the role of triggering centers [Figs. 4(a) and 4(b)]. Upon further decreasing the temperature to 476 K, the plane wave fronts start to become unstable. Upon collision with a defect, the wave fronts break apart, with the free ends curling up into pairs of rotating spirals. This situation is depicted in Fig. 4(c). Here, plane wave fronts and spiral waves coexist. At lower temperature ($T=474.5$ K), the plane wave fronts have disappeared and only small spirals with one or two windings populate the surface as demonstrated by Fig. 4(e). Upon further decreasing the temperature to 472 K, the spirals become unstable and spontaneously break up into fragments. A typical image showing the spiral fragments is displayed in Fig. 4(f). At 470 K, the medium is largely spatially homogeneous and one only observes local outbursts in the reacting medium. Dark areas, which correspond to a high CO-coverage and therefore low reactivity, form and dissolve again. Finally, at 469 K, a stable uniform state of the surface is reached.

The spatiotemporal patterns just described have also been characterized by their local time series. This was done by integrating the PEEM intensity in a small window of 20×20 μm^2 size. The time series obtained this way are displayed in Fig. 7, together with the corresponding power spectra. As a general trend one first notes, that during the

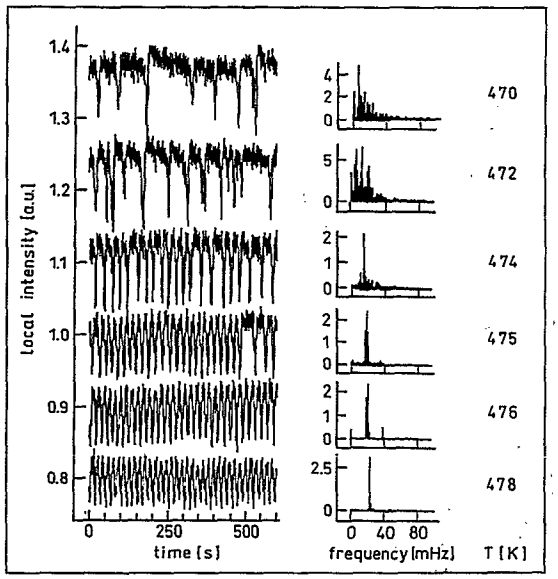

FIG. 7. Local time series and corresponding power spectra for the spatial patterns shown in Fig. 4. The time series were taken by integrating the intensity of an area of 20×20 μm^2 in the PEEM images. Experimental conditions were $p_{NO}=4\times10^{-6}$ mbar and $p_{CO}=4\times10^{-6}$ mbar.

whole scenario the frequency shifts to lower values, while the power spectrum simultaneously broadens. As expected, the periodic wave trains seen at $T=478$ K give rise to a single sharp frequency component slightly above ≈20 mHz. With the formation of spirals some broadening and a small shift to lower frequency occurs, but the spectrum is still dominated by a single main frequency near 20 mHz. A noticeable change in the spectra is observed when the spirals start to break up. The frequency spectrum then no longer displays a few distinct lines, but one observes a broad maximum which is strongly asymmetric in its weight towards the low frequency side. This asymmetry increases further with decreasing temperature.

The existence of a continuous frequency spectrum for $T<472$ K indicates turbulent behavior in the T-range where spiral breakup and local outbursts are observed. For the characterization of spatiotemporal turbulence no rigorous criteria exist, but a lack of long range spatial correlations is an obvious prerequisite. In order to test this criterium for the data presented here, a spatial two-point correlation was computed for two local time series recorded in two windows of 20 μm×20 μm size and ≈200 μm distance apart. The results displayed in Fig. 8 demonstrate, that the spatial correlation decays within only 1–2 cycles for the chaotic data of Fig. 7, while it decays only very slowly over a large number of cycles in the case of the periodic time series above $T\approx474$ K. The decay in the latter case can be attributed to the noise level in the data.

IV. DISCUSSION

A. The oscillation mechanism

Based upon the vacancy mechanism for NO dissociation and the properties of the 1×1⇔hex SPT, a mathematical model for the NO+CO reaction on Pt(100) has been developed, which reproduces fairly well the hysteresis behavior of the reaction and the two existence ranges for kinetic oscillations.[3,5] The model, however, predicts a phase relationship between the amount of hex reconstruction and the CO_2 production rate which is opposite to that observed in the experiment. Moreover, it yields a temperature dependence for the oscillation frequency that is also just the opposite of the trend in the experimental data in Fig. 6, i.e., the model predicts a frequency rise with decreasing temperature. Therefore, the existing model for oscillations in the NO+CO reaction on Pt(100) clearly needs to be improved in order to correctly reproduce the experimental data. Such an improved model is currently in progress. Yet, in the following we only briefly discuss some of the qualitative features of the improved model in as far as they are relevant for a better understanding of the present experimental findings.

Previous LEED experiments and also the present PEEM investigations indicate, that the reaction rate correlates with the degree of reconstruction. The same phase relationship follows from an *in situ* Fourier transform infrared (FTIR) spectroscopy investigation of the oscillatory NO+CO reaction on Pt(100), since it was found that the maximum intensity of the CO stretch frequency, and hence the maximum in CO coverage, correlates with the minimum of the reaction rate.[21] Accordingly, the minimum in the amount of hex reconstruction coincides with the minimum in CO_2 production. Moreover, no NO was detectable in those experiments during oscillations in the upper T-range.

Since the 1×1-surface is the one that is active in NO dissociation, while the hex-phase is ineffective in that respect, the correlation above seems to be in contradiction to the experimental facts.[2,3,11,13] However, the hex-phase, which is formed at relatively low temperature, is structurally imperfect, and since defects are very efficient in dissociating NO, a substantial level of catalytic activity can be present on a nonannealed hex-phase.[3,22,23] For understanding the correlation between hex reconstruction and catalytic activity in the oscillations, the role of the defects must therefore be examined more closely. A strongly simplified picture of an oscillatory cycle illustrating the role of defects is presented in the following.

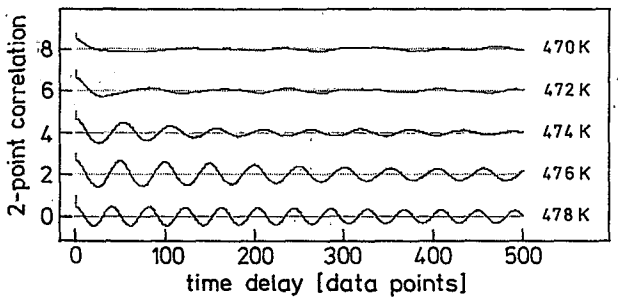

FIG. 8. Spatial two-point correlation functions for some of the spatiotemporal patterns shown in Fig. 4. The functions were calculated using time series like those shown in Fig. 7 at two different spots on the surface separated by ≈200 μm. Experimental conditions were $p_{NO}=4\times10^{-6}$ mbar and $p_{CO}=4\times10^{-6}$ mbar.

Starting with a completely hex-reconstructed surface, CO adsorption initiates the nucleation of 1×1-CO islands (coadsorbed with some NO). These islands are stable, since the reaction is locally inhibited by the relatively high adsorbate coverage, which inhibits the NO dissociation. Above a critical radius, the islands become unstable and the autocatalytic reaction between NO and CO leads to a rapid removal of the adsorbate. Thus, bare 1×1-islands are created, which are very reactive, and even as the 1×1-area is converted into hex-phase, a high level of catalytic activity will remain as a consequence of the large amount of structural imperfections. Only as the defect concentration decreases due to thermal annealing, will the catalytic activity drop. This will trigger the formation of 1×1-CO islands and the oscillation cycle starts again. This mechanism explains why the catalytic activity in the oscillations correlates with the degree of hex-reconstruction.

B. Synchronization mechanism

Synchronization in the upper T-range for oscillations is transmitted via partial pressure changes in the gas-phase. This mode is ineffective at lower temperature where oscillations in the NO+CO reaction exist only on a local scale.[6,9] Since these unsynchronized oscillations take place on a pure 1×1-substrate without any involvement of the 1×1⇔hex SPT, a close-lying assumption is, that the 1×1⇔hex SPT is essential for synchronizing the oscillations. This conclusion is further supported by the following experimental observations.

In the NO+NH_3 reaction on Pt(100), kinetic oscillations were detected, which similar to the NO+CO reaction, proceed spatially uniformly on a largely hex-reconstructed surface.[24–26] As with decreasing temperature a larger amount of the hex-reconstructed surface is converted into the 1×1-phase, global coupling breaks down. The rate oscillations disappear and, again similar to NO+CO, the surface is only oscillating on a local scale.[26]

These observations strongly support the idea, that common to all three oscillatory NO-reduction reactions on Pt(100), NO+CO, NO+H_2, and NO+NH_3, the 1×1⇔hex SPT synchronizes the local oscillations in these systems. The role of the SPT in the synchronisation mechanism can be depicted in the following way: The hex⇒1×1 SPT proceeds over the nucleation and growth of 1×1-(CO/NO) islands, with the nucleation process being controlled by critical adsorbate coverages of CO and NO on the hex-phase ($\theta_{CO,crit}\approx 0.05$).[14,15,27] Under oscillatory conditions, the (p,T)-parameters are such, that in an adsorption/desorption equilibrium of the gases with the hex-phase, the adsorbate coverages on the hex-phase are always close to θ_{crit}. It is thus evident, that even small partial pressure variations can then have a pronounced influence on the surface reaction. The variations modify the nucleation rate of 1×1-islands, thereby synchronizing the oscillating surface reaction.

The breakdown of synchronization at lower temperatures, which led to the collapse of the rate oscillations, is apparently a phenomenon of more general interest. For this reason, simulations of this transition have been conducted with a modified complex Ginzburg–Landau (CGL) equation, since this equation is known to exhibit universal validity in the vicinity of a Hopf bifurcation.[28] The simulations were able to reproduce the discontinuous breakdown of global coupling occurring when some defects (at least one) become supercritical, i.e., when the frequency difference between the defect and the bulk exceeds a certain threshold.[10,29] The only qualitative difference to the experiment was, that the simulated transition always exhibited a strong hysteresis upon parameter variation, while such an effect was absent in the experiments. The reason for this discrepancy can be sought in the experimental procedure, since a very small, but finite, T-jump ($\Delta T<1$ K) always had to be used to vary the temperature. From previous investigations, however, we know that the NO+CO reaction is extremely sensitive to T-variations and therefore even small T-jumps will have an additional strongly synchronizing effect, which is not accounted for in the CGL model.

The breakdown of global coupling associated with spatial pattern formation has also been studied with PEEM in another oscillatory reaction, namely the NO+NH_3 reaction on Pt(100).[26] Interestingly, however, the scenario is qualitatively different from the one in the NO+CO reaction. In the NO+NH_3 reaction, the transition from the synchronized oscillating state to spatiotemporal pattern formation does not take place in the abrupt manner observed in the NO+CO reaction, but one has coexistence of synchronized oscillations and spatial patterns over a finite temperature range. Fluctuating islands and, at lower temperature, target patterns and spiral waves form, which cover only part of the surface area while the rest is still oscillating in a synchronized way. The vanishing amplitude of the rate oscillations then finally carries the system into a regime of spatiotemporal turbulence.

C. Deterministic chaos

A remarkable effect in the NO+CO reaction on Pt(100) is the occurrence of a Feigenbaum scenario at the upper T-boundary of the oscillatory range. Such a scenario has also been found in two other oscillatory reactions on single crystal surfaces, namely in the CO+O_2 reaction on Pt(110) and in the NO+H_2 reaction on Pt(100).[17,18,30] Although the embedding dimension was shown to be small ($\leqslant 5$) for both systems, so far all attempts to reproduce the chaotic behavior with a set of realistic differential equations were without success. The origin of low-dimensional deterministic chaos in oscillatory surface reactions is therefore still unclear and, in particular, the role of the spatial degrees of freedom remains an open question.

In catalytic CO oxidation on Pt(110), a detailed analysis of the aperiodic data has been conducted, and a bifurcation diagram for the transition to chaos could be established.[17,18] For Pt(100)/NO+H_2, a similar analysis of the chaotic time series was carried out, but the transition to chaos occurred in such a small parameter range that no experimental bifurcation diagram fo the period-doubling sequence could be determined.[30]

With respect to modelling, the present system has the advantage, that within the resolution of the PEEM instrument (≈ 1 μm), no spatiotemporal patterns were detectable during

the Feigenbaum transition. Accordingly, a mathematical description with ordinary differential equations (ODE's) should be possible for the chaotic behavior of the NO+CO reaction. For the existing six-variable model of the NO+CO reaction on Pt(100), no chaotic oscillations were found, but one can expect, that with the introduction of the defect concentration as an additional variable, the dynamics of the reaction system would become more complex, and possibly also exhibit chaos. This is one possible way through which chaos could arise, but an alternative explanation based on synchronization effects is favored by the authors following the reasoning given below.

Since chaos in the NO+H_2 reaction on Pt(100) occurs under conditions very similar to those of the NO+CO reaction, it is rather unlikely that details of the chemistry play any important role in the development of chaotic behavior. Rather, one might suspect that a mechanistic element common to both systems plays a decisive role and such a common element could be given by the 1×1⇔hex SPT. Since the SPT synchronizes the rate oscillations, a plausible mechanism for the development of chaotic oscillations could be based on the synchronization process.

Synchronization requires partial pressure variations of finite amplitude. Since, however, the oscillation amplitude grows continuously from the stationary state (see Fig. 1), there has to be a transition which connects the state of unsynchronized local oscillations and zero rate amplitude to synchronized oscillations with a finite rate amplitude. If one depicts the individual oscillators as small 1×1-CO/NO islands (<1 μm), which randomly nucleate and dissolve on the hex-phase, the above depicted mechanism is not in contradiction with PEEM measurements, which show spatial homogeneity. The transition from unsynchronized to synchronized oscillations can be visualized in the following way.

Starting with the unsynchronized state, in which 1×1-islands randomly nucleate and dissolve, the reaction rate will first exhibit a stationary value. As with decreasing temperature the nucleation rate increases strongly, the nucleating islands synchronise via the gas-phase and as a result of this process, one obtains finite amplitude rate oscillations. The crucial question is, however, whether such a mechanism can in fact lead to a Feigenbaum scenario and finally to deterministic chaos, since these occur typically in low-dimensional systems and not in systems involving a large number of coupled oscillators as it is the case here.

There is some support for the idea, that synchronization can in fact cause deterministic chaos from theory and from experiment. In a study with probabilistic cellular automatons (CA's), Mikhailov *et al.* showed that, if a large number of randomly oscillating cells are globally coupled together, a spatially synchronized state can develop, which in its temporal behavior displays deterministic chaos.[31] In addition, they find a Feigenbaum scenario, leading from chaotic oscillations to regular period-1 oscillations. The surprising fact in these simulations is, that in the chaotic state the system reacts spatially uniformly, while only the temporal signal exhibits aperiodic behavior. On the experimental side, STM studies have shown that the nucleation of the 1×1-phase during the adsorption of NO and CO onto the hex-reconstructed Pt(100) surface occurs homogeneously.[32] With homogeneous nucleation occurring, the reaction rate should depend strongly on the degree of supersaturation and thus be sensitive to small partial pressure variations, as is required by the mechanism depicted above.

From the present experimental data it is not possible to unambiguously discriminate between the two alternative explanations for the emergence of chaotic behavior in the NO+CO reaction on Pt(100), and therefore both routes should be considered as possible mechanisms. One can, however, expect to be able to decide such a question by simulations with appropriate models. Such simulations are currently underway.

D. Spatiotemporal patterns

Excitable systems can be distinguished from oscillatory systems by the existence of an excitation threshold which has to be surmounted to induce an excursion of the system in phase space.[33] Yet, in spatially distributed systems, this distinction can be effaced by diffusional coupling between adjacent local oscillators, which can trigger an early transition between the different branches of an oscillatory cycle, thus giving rise to an apparent excitation threshold.[33–35]

Although the distinction between oscillatory and excitable media is therefore not sharply defined for spatially distributed systems, the experimentally observed behavior of the NO+CO reaction below T_2 can be best understood in terms of such a transition. The existence of spiral waves as well as the breaking of parallel reaction fronts can in principle be explained by both oscillatory and excitable system dynamics. The observation of increasingly localized reaction outbursts at low T, however, clearly indicates an excitable medium and therefore, at some point during the transition from regular parallel waves to the breaking of spiral waves, the intrinsic system dynamics change from oscillatory to excitable. The increasing localization of the reaction outbursts, the decreasing lifetime of these outbursts, and the increasing irregularity of the lag time between them can then be explained by an excitability, that decreases continuously with decreasing temperature.

V. CONCLUSIONS

Sustained rate oscillations were obtained in the NO+CO reaction on Pt(100) by applying special care to the preparation of the single crystal surface. The rate oscillations proceed spatially homogeneously on a largely hex-reconstructed surface, with spatial synchronization during the oscillations being achieved via gas-phase coupling. A synchronization mechanism has been suggested, which is based on the critical dependence of the lifting of the hex-reconstruction on the partial pressures of the educt gases. A bifurcation diagram for the oscillatory T-window has been established. At the high-T end of the oscillatory range, the oscillations set in through a Feigenbaum scenario, i.e., they develop from deterministic chaos to regular period-1 oscillations. A model

has been proposed for the appearance of deterministic chaos in the NO+CO reaction, based on synchronization effects between individual local oscillators.

At the low-T boundary of the existence range for rate oscillations, a discontinuous transition to a steady state reaction rate takes place associated with the appearance of target patterns. As substantiated by modeling with the complex Ginzburg–Landau equation, defects play a decisive role in this transition. As defects become supercritical, they act as nuclei for the breakdown of synchronization via gas-phase coupling. Upon further decreasing the sample temperature, the spatial patterns change from parallel wave trains to increasingly irregular patterns. This sequence can be described as a transition from an oscillatory to an excitable medium. Finally, with decreasing excitability, a regime of spatiotemporal turbulence is reached.

ACKNOWLEDGMENTS

Technical assistance by S. Wasle is gratefully acknowledged. G. V. thanks the "Stiftung Stipendienfonds des VCI" for financial support through a Kékulé-scholarship.

[1] S. P. Singh-Boparai and D. A. King, in Proceedings of the 4th International Congress on Surface Science, Cannes, 1980, pp. 403.
[2] S. B. Schwartz and L. D. Schmidt, Surf. Sci. **206**, 169 (1988).
[3] T. Fink, J.-P. Dath, R. Imbihl, and G. Ertl, J. Chem. Phys. **95**, 2109 (1991).
[4] J.-P. Dath, T. Fink, R. Imbihl, and G. Ertl, J. Chem. Phys. **96**, 1582 (1992).
[5] R. Imbihl, T. Fink, and K. Krischer, J. Chem. Phys. **96**, 6236 (1992).
[6] G. Veser and R. Imbihl, J. Chem. Phys. **96**, 7155 (1992).
[7] J. W. Evans, H. H. Madden, and R. Imbihl, J. Chem. Phys. **96**, 4805 (1992).
[8] G. Veser, P. A. Thiel, and R. Imbihl, J. Phys. Chem. (in press).
[9] G. Veser and R. Imbihl, J. Chem. Phys. **100**, 8483 (1994).
[10] G. Veser, F. Mertens, A. Mikhailov, and R. Imbihl, Phys. Rev. Lett. **71**, 935 (1993).
[11] T. Fink, J.-P. Dath, M. R. Bassett, R. Imbihl, and G. Ertl, Surf. Sci. **245**, 96 (1991).
[12] W. Engel, M. E. Kordesch, H. H. Rotermund, S. Kubala, and A. von Oertzen, Ultramicrosc. **36**, 148 (1991).
[13] H. P. Bonzel, G. Brodén, and G. Pirug, J. Catal. **53**, 96 (1978).
[14] R. J. Behm, P. A. Thiel, P. R. Norton, and G. Ertl, J. Chem. Phys. **78**, 7437 (1983).
[15] P. A. Thiel, R. J. Behm, P. R. Norton, and G. Ertl, J. Chem. Phys. **78**, 7448 (1983).
[16] M. J. Feigenbaum, J. Stat. Phys. **19**, 25 (1978).
[17] M. Eiswirth, K. Krischer, and G. Ertl, Surf. Sci. **202**, 565 (1988).
[18] M. Eiswirth, T.-M. Kruel, G. Ertl, and F. W. Schneider, Chem. Phys. Lett. **193**, 305 (1992).
[19] M. J. Feigenbaum, J. Stat. Phys. **21**, 669 (1979).
[20] F. Takens, in *Dynamical System and Turbulence*, edited by D. A. Rond and L. S. Young (Springer, Berlin, 1981), p. 366.
[21] P. Gardner, R. Martin, R. Nalezinski, and A. M. Bradshaw (unpublished).
[22] J. L. Gland, Surf. Sci. **71**, 327 (1978).
[23] Y. Uchida, R. Imbihl, and G. Lehmpfuhl, Surf. Sci. **275**, 253 (1992).
[24] S. J. Lombardo, F. Esch, and R. Imbihl, Surf. Sci. **271**, L367 (1992).
[25] M. F. H. van Tol, J. Siera, P. D. Cobden, and B. E. Nieuwenhuys, Surf. Sci. **274**, 63 (1992).
[26] G. Veser, F. Esch, and R. Imbihl, Catal. Lett. **13**, 371 (1992).
[27] P. Gardner, R. Martin, M. Tüshaus, and A. M. Bradshaw, J. Electron Spectrosc. Relat. Phenom. **54/55**, 619 (1990).
[28] Y. Kuramoto, *Chemical Oscillations, Waves and Turbulence* (Springer, Berlin, 1984).
[29] F. Mertens, R. Imbihl, and A. S. Mikhailov, J. Chem. Phys. **99**, 8668 (1993).
[30] P. D. Cobden, J. Siera, and B. E. Nieuwenhuys, J. Vac. Sci. Technol. A **10**, 2487 (1992).
[31] O. A. Druzhinin and A. S. Mikhailov, Sov. Phys. Quantum Electron. Radiophys. **32**, 334 (1989).
[32] E. Ritter, R. J. Behm, G. Pötschke, and J. Wintterlin, Surf. Sci. **181**, 403 (1987).
[33] A. S. Mikhailov, *Foundations of Synergetics* (Springer, Berlin, 1991).
[34] P. Ortoleva and J. Ross, J. Chem. Phys. **60**, 5090 (1974).
[35] P. Ortoleva and J. Ross, J. Chem. Phys. **63**, 3398 (1975).